

An upper extremity kinematic model for evaluation of hemiparetic stroke

Brooke Hingtgen^{a,c}, John R. McGuire^b, Mei Wang^{a,c}, Gerald F. Harris^{a,c,*}

^aDepartment of Biomedical Engineering, Marquette University, Milwaukee, WI, USA

^bDepartment of Physical Medicine and Rehabilitation, Medical College of Wisconsin, Milwaukee, WI, USA

^cOrthopaedic and Rehabilitation Engineering Center, Marquette University and Medical College of Wisconsin, Milwaukee, WI, USA

Accepted 10 January 2005

Abstract

Quantification of rehabilitation progress is necessary for accurately assessing clinical treatments. A three-dimension (3D) upper extremity (UE) kinematic model was developed to obtain joint angles of the trunk, shoulder and elbow using a Vicon motion analysis system. Strict evaluation confirmed the system's accuracy and precision. As an example of application, the model was used to evaluate the upper extremity movement of eight hemiparetic stroke patients with spasticity, while completing a set of reaching tasks. Main outcome measures include kinematic variables of movement time, range of motion, peak angular velocity, and percentage of reach where peak velocity occurs. The model computed motion patterns in the affected and unaffected arms. The unaffected arm showed a larger range of motion and higher angular velocity than the affected arm. Frequency analysis (power spectrum) demonstrated lower frequency content for elbow angle and angular velocity in the affected limb when compared to the unaffected limb. The model can accurately quantify UE arm motion, which may aid in the assessment and planning of stroke rehabilitation, and help to shorten recovery time.

© 2005 Elsevier Ltd. All rights reserved.

Keywords: Kinematics; Upper extremity; Biomechanics; Rehabilitation; Stroke

1. Introduction

The focus of this work is the design and evaluation of a three-dimensional (3D) upper extremity (UE) motion assessment system to quantify progress of stroke rehabilitation. The nature of arm motion is different from human gait, because it is variable and complex (Rau et al., 2000; Yang et al., 2002). No standard activities exist for the arm. In order for arm motion analysis to become routinely used for rehabilitation assessment, a set of discriminating tasks should be established (Yang et al., 2002).

Many previous approaches to analyze upper extremity motion did not allow a wide range of clinical applications. Some were invasive (Hogfors et al., 1991; Schmidt et al., 1999) or the setup restricted movement (Andrews and Youm, 1979; Peterson and Palmerud, 1996; Schmidt et al., 1999). Other models simplify the upper extremity by neglecting some degree of freedom (Schmidt et al., 1999; Biryukova et al., 2000; Michaelsen et al., 2001).

Several studies have examined reaching tasks in stroke subjects, but few incorporate upper extremity motion analysis (Kemper et al., 2002). The few existing UE models lack validation, all degrees of freedom and 3D Euler joint angles (Adamovich et al., 2001; Michaelsen et al., 2001). Data obtained from these models is often collected from a small sample population and with few cameras, resulting in marker dropout and requiring motion estimates (Yang et al., 2002).

*Corresponding author. Department of Biomedical Engineering, Marquette University, Academic Support Facility, Suite 105, 735N. 17th Street, Milwaukee, WI 53233, USA. Tel.: +1 414 805 7456.

E-mail addresses: brooke.hingtgen@mu.edu (B. Hingtgen), geraldharris@msn.com (G.F. Harris).

Accurate quantitative assessment is essential in monitoring recovery progress during stroke rehabilitation. The objective of this study is to develop and validate a 3D UE motion assessment system to quantify progress during stroke rehabilitation. An application of this system that compares kinematics of the elbow joint between the affected and unaffected arms is presented.

2. Methods

2.1. Kinematic model

The upper extremity model consists of the five following segments: (1) trunk, (2) right upper arm, (3) right forearm, (4) left upper arm, and (5) left forearm. The segments are connected by a three degree-of-freedom shoulder joint (glenohumeral joint) and a two-degree of freedom elbow joint. This constrained varus and valgus at the elbow. Fourteen passive markers are placed on bony anatomical landmarks to define the segments and minimize skin motion. The joint centers and joint axes are defined using subject specific anthropometric measurements and markers. Pronation and supination of the forearm is expressed through motion defined at the elbow. Vicon BodyBuilder V3.55 (Vicon Motion Systems, Ltd., Oxford, England) was used for the development of the model. Euler angles are used to determine the 3D joint angles (Chao, 1980; Grood and Suntay, 1983; Ramakrishnan and Kadaba, 1991; Harris and Smith, 1996). A series of Euler rotations, sequenced Y-Z-X, were used to express the joint angles of the distal segment with respect to the proximal segment, utilizing each segment’s local coordinate system. The trunk segment was described with reference to the lab coordinate system. A 15-camera Vicon 524 system, with a 120 Hz capturing rate, recorded the UE motion patterns.

2.1.1. Joint centers

In defining the model, it was first necessary to determine the joint center locus for the trunk, shoulder,

elbow, and wrist. The position of the joint center served as the origin for each segment’s local coordinate system (Fig. 1). All joints were assumed to have fixed centers of rotation. Marker nomenclature and corresponding bony landmarks are clarified in Table 1.

Trunk: The trunk was defined using markers at the right and left acromion processes, spinous process C7, sternal notch, and the right and left anterior–superior iliac spine. The origin of the trunk segment is located at the center of the acromion markers,

$$\bar{i}_c = \frac{1}{2}(\bar{m}_{racr} + \bar{m}_{lacr}), \tag{1}$$

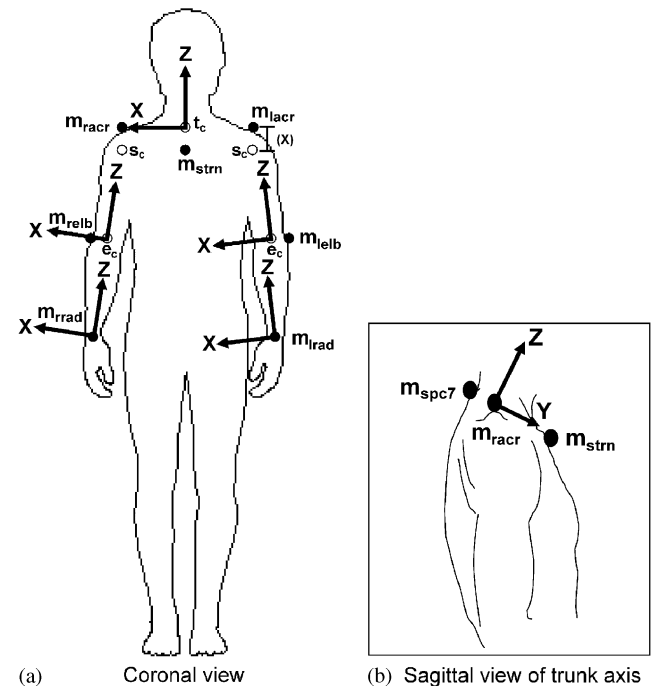


Fig. 1. Local coordinate axes systems for the upper extremity model, (a) coronal view, (b) sagittal view of trunk axis. Markers are shown as black circles and joint centers are shown as open circles. Axes follow the convention X: flexion/extension, Y: adduction/abduction, Z: axial rotation. The distance (x) was determined by measuring the circumference of the shoulder around the acromion and axilla.

Table 1
Marker names, locations and corresponding segments

Marker: <i>m</i> (subscript)	Location	Segment
spc7	Spinous process of C7 vertebra	Trunk
strn	Sternal notch	Trunk
r/lasis	R/L anterior superior iliac spine	Trunk
r/lacr	R/L acromion	Trunk and upper arm
r/lhum	R/L humerus	Upper arm
r/lelb	R/L olecranon	Upper arm and forearm
r/lrad	R/L radial styloid	Forearm
r/luln	R/L ulnar styloid	Forearm

where \bar{i}_c is the location of the trunk center, having x , y , and z coordinates, and \bar{m}_i refers to the marker location, where $i = \text{marker}$ (Table 1).

Shoulder: The glenohumeral joint was modeled as a ball and socket joint, with no translation of the rotation center of the humerus. The joint center was located at the center of the humeral head (Poppen and Walker, 1976; Veeger et al., 1997; Wang et al., 1998; Biryukova et al., 2000; Bachschmidt et al., 2001; Roux et al., 2002). To determine the joint center location, the circumference of the shoulder, around the acromion and axilla was measured for each subject. From this approximated circular measurement, the radius of the shoulder was calculated (x). The joint center was then located inferiorly from the acromion, at the measured distance (x). It was defined as the following:

$$\bar{s}_c = m_{\text{acr}} - (x)(\bar{i}_z), \quad (2)$$

where \bar{i}_z is the z -axis unit vector of the trunk coordinate system, \bar{s}_c is the 3D location of the shoulder center, and \bar{m}_i refers to the marker location, where $i = \text{marker}$.

Elbow: The elbow joint center was assumed to lie anterior to the olecranon process. It was subject specific and determined by using the measured width of the elbow. The computations used an offset measurement of the half sum of the elbow width and the marker diameter,

$$e_{\text{offset}} = \frac{1}{2}(w + d), \quad (3)$$

where e_{offset} is the offset measurement, w is the elbow width, and d is the marker diameter.

A temporary axis, \bar{e}_1 , was used to define point, \bar{p} , anterior to the left elbow marker:

$$\bar{e}_{1,y} = \frac{\bar{m}_{\text{spc7}} - \bar{m}_{\text{lelb}}}{|\bar{m}_{\text{spc7}} - \bar{m}_{\text{lelb}}|}, \quad (4)$$

$$\bar{e}_{1,x} = \frac{(\bar{m}_{\text{hum}} - \bar{m}_{\text{lelb}})}{|\bar{m}_{\text{hum}} - \bar{m}_{\text{lelb}}|} \times \bar{e}_{1,y}, \quad (5)$$

$$\bar{p} = \bar{m}_{\text{lelb}} + 10(\bar{e}_{1,x}), \quad (6)$$

where $\bar{e}_{i,j}$ is a unit vector, where $i = 1, 2$, which signifies the axis number, and $j = x, y, z$, which signifies the vector.

A second temporary axis, \bar{e}_2 , was used to create a system for locating the left elbow joint center, \bar{e}_c , medial to the elbow marker, where

$$\bar{e}_{2,x} = \frac{\bar{p} - \bar{m}_{\text{lelb}}}{|\bar{p} - \bar{m}_{\text{lelb}}|}, \quad (7)$$

$$\bar{e}_{2,y} = \frac{(\bar{m}_{\text{hum}} - \bar{m}_{\text{lelb}})}{|\bar{m}_{\text{hum}} - \bar{m}_{\text{lelb}}|} \times \bar{e}_{2,x}. \quad (8)$$

The left elbow joint center, \bar{e}_c , is defined as

$$\bar{e}_c = \bar{m}_{\text{lelb}} - (e_{\text{offset}})\bar{e}_{2,y}, \quad (9)$$

using the elbow marker and a distance of the elbow offset in the y -direction of the second temporary vector.

The right elbow joint center was found in a similar manner.

Wrist: The wrist joint center was located halfway between the radial and ulnar styloid processes:

$$\bar{w}_c = \frac{1}{2}(\bar{m}_{\text{rad}} + \bar{m}_{\text{uln}}), \quad (10)$$

where \bar{w}_c is the center of the wrist and \bar{m}_i refers to the marker location, where $i = \text{marker}$.

2.1.2. Segmental coordinate systems

Segment coordinate systems were used to determine the joint angles (Fig. 1). The relative motion between distal and proximal local coordinate systems was determined. Right-handed coordinate systems were constructed following clinical convention (Rab et al., 2002). It follows that the X -axis is directed laterally to the right, Y -axis is directed forward (anteriorly), and the Z -axis directed upward (superiorly).

Trunk: Vectors defining the principal directions of the trunk coordinate system $\{T\}$ are denoted as \bar{X}_T , \bar{Y}_T , and \bar{Z}_T .

$$\bar{X}_T = \frac{\bar{m}_{\text{racr}} - \bar{m}_{\text{lacr}}}{|\bar{m}_{\text{racr}} - \bar{m}_{\text{lacr}}|}, \quad (11)$$

$$\bar{Z}_T = \frac{(\bar{i}_c - \bar{m}_{\text{strn}})}{|\bar{i}_c - \bar{m}_{\text{strn}}|} \times \bar{X}_T, \quad (12)$$

where \bar{i}_c is the origin of the trunk coordinate system.

Upper arm: Unit vectors giving the principal directions of the upper arm coordinate system $\{UA\}$ are denoted as \bar{X}_{UA} , \bar{Y}_{UA} , and \bar{Z}_{UA} . The following vectors define the left upper arm axis:

$$\bar{Z}_{UA} = \frac{\bar{s}_c - \bar{e}_c}{|\bar{s}_c - \bar{e}_c|}, \quad (13)$$

$$\bar{Y}_{UA} = \frac{(\bar{m}_{\text{lelb}} - \bar{e}_c)}{|\bar{m}_{\text{lelb}} - \bar{e}_c|} \times \bar{Z}_{UA}, \quad (14)$$

where \bar{s}_c and \bar{e}_c are the origin of the shoulder and elbow coordinate systems, respectively.

Forearm: The unit vectors giving the principal directions of the forearm coordinate system $\{FA\}$ are denoted as \bar{X}_{FA} , \bar{Y}_{FA} , and \bar{Z}_{FA} . The axes of the left forearm is defined as

$$\bar{Z}_{FA} = \frac{\bar{e}_c - \bar{w}_c}{|\bar{e}_c - \bar{w}_c|}, \quad (15)$$

$$\bar{X}_{FA} = \frac{(\bar{s}_c - \bar{w}_c)}{|\bar{s}_c - \bar{w}_c|} \times \bar{Z}_{FA}, \quad (16)$$

where \bar{e}_c , \bar{w}_c , and \bar{s}_c are the origin of the elbow, wrist, and shoulder coordinate systems, respectively.

2.2. Evaluation

Root mean square error (RMS) and standard deviation of the UE model were examined statically and

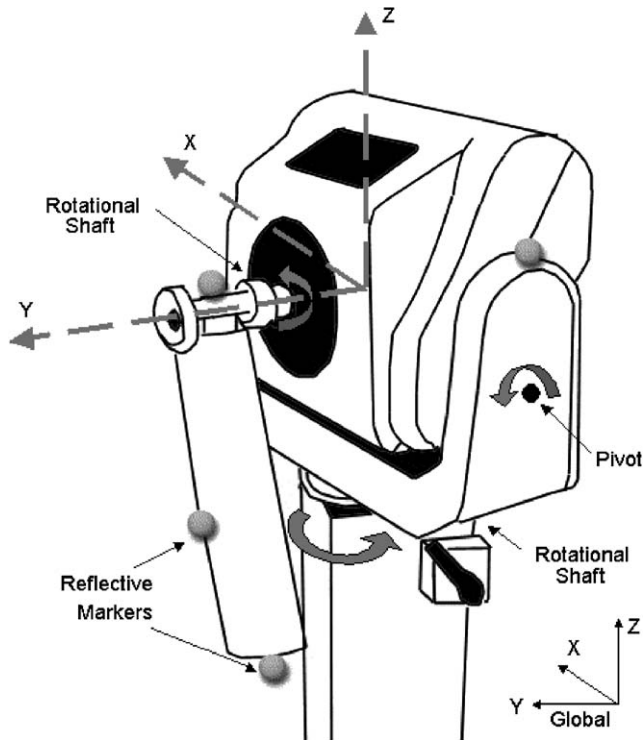


Fig. 2. Biodex System-3 setup for validation testing using simulated segment with reflective markers.

dynamically. Static linear testing involved placing four markers on a fixed segment to represent the shortest (50 mm), intermediate (150 mm), and longest (300 mm) distances of UE marker placement. To assess dynamic linear motion, the segment was moved throughout the capture volume at an average arm speed based on stroke pilot data, while Vicon recorded the marker positions. Dynamic angular testing was completed using a Biodex System-3 (Biodex Medical Systems, Inc., New York). A simulated segment with three markers was attached to the Biodex arm and four markers were placed on the stationary chassis (Fig. 2). The Biodex moved through a range of 230° at 20° per second, based on pilot data from stroke patients.

There were times during the Biodex motion that acceleration and deceleration occurred. A window of time existed at which constant velocity (20° per second) was considered for the analysis. The range of motion was set from zero to 230° , however, there was a window of 200° where angular velocity was constant. Thus, four measurements per trial (5 trials) were taken throughout this window to determine accuracy and standard deviation. The variables collected from the Biodex outputs that were of interest in this study include time, angular position (range = 330° and accuracy = $\pm 1^\circ$ of rotation), and angular velocity (range = $1\text{--}500^\circ$ per second and accuracy = $\pm 1^\circ$ per second).

RMS error was calculated to determine system accuracy, as follows:

$$\text{RMS error} = \sqrt{\frac{\sum (x_i - d)^2}{n}}, \quad (17)$$

where x_i is the measured value, d is the actual value, and n is the number of samples. Percent RMS error was then determined by taking the RMS error divided by the respective actual value. Standard deviation was computed to evaluate system precision, using the following equation:

$$\text{Standard deviation} = \sqrt{\frac{n \sum x_i^2 - (\sum x_i)^2}{n(n-1)}}, \quad (18)$$

where n is the number of samples, and x_i is the measured value.

2.3. Patient population

The study protocol was approved by the Institutional Review Boards at the Medical College of Wisconsin and Marquette University. Eight adult subjects of 51.3 ± 14.8 years volunteered and gave written informed consent to participate in this study. The patient population included three females and five males ranging from 22 to 69 years. Subjects had experienced a stroke and were scheduled to receive BOTOX® (Botulinum Toxin Type A) injections as part of their routine clinical treatment. Subjects must have scored a one (slight increase in tone, giving a catch when the limb is moved in flexion or extension) or four (rigid in flexion or extension) on the Ashworth scale in at least two of the following muscle groups: shoulder adductors, elbow flexors, elbow extensors, pronators, wrist flexors, and finger and/or thumb flexors/adductors. Additionally, a Medical Research Council (MRC) manual muscle strength test must have been grade 1–4 (1—flicker or trace of contraction; 2—active movement possible only with gravity eliminated; 3—active movement against gravity but not resistance; 4—active movement against resistance and gravity) in the shoulder abductors, and elbow and finger flexors/extensors (Tzvetanov et al., 2003).

2.4. Experimental setup

The subjects were seated in a chair at a therapy table. The chair was a non-swivel, stationary, high-back chair, positioned at 90° upright (Sammons Preston Rolyan, Bolingbrook, IL). The chair was adjusted so that subjects were seated with their feet flat on the floor with a knee angle of 90° . The table was a height adjustable, cutout therapy table measuring 3 ft \times 5 ft (Sammons Preston Rolyan, Bolingbrook, IL).

A reaching target was placed directly in front of the subjects during the tasks (Fig. 3). To begin, the subjects

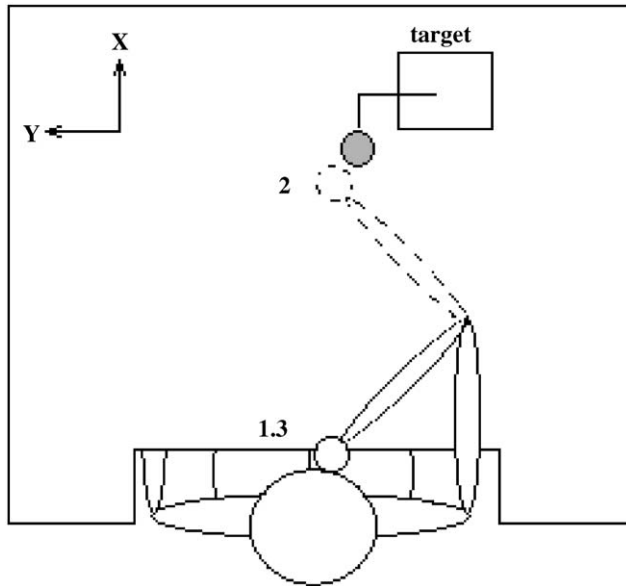


Fig. 3. Subject seated at a therapy table reaching to a target placed directly in front of them (from above). The subject (1) starts with the hand against the sternum, (2) reaches at a comfortable (self-selected) pace to the target, and (3) ends with the hand at the sternum.

were verbally instructed to place their hand against their sternum. Next, the patients were instructed to reach as far as they can at their own pace to the target directly in front of them. After reaching the target, the subjects end the reaching cycle with their hand against their sternum. A complete reaching cycle is defined as elbow flexion (beginning) to elbow extension (midpoint) and back to elbow flexion (end). Each task was successfully completed three times per arm. To prevent fatigue, the subjects switched between the unaffected and affected arm.

2.5. Data collection and analysis

Vicon Workstation (Vicon Motion Systems, Ltd., Oxford, England) was used to anatomically label, filter (Woltring, 1986), and apply the UE model. The output data included marker positions, joint positions, and joint angles throughout the reaching cycle.

The analysis of elbow flexion/extension during reaching at the subject's self-selected speed was presented here. The data was exported to Matlab (The MathWorks, Inc., Natick, MA) for further analysis. First, elbow range of motion in the sagittal plane was computed for the affected arm and unaffected arm of each patient. Then, angular velocity of the elbow was calculated.

Calculations of angular velocity were completed using the following equations (Vaughan et al., 1992):

$$\omega_x = \dot{\theta}_y \cdot \sin(\theta_z) + \dot{\theta}_x, \quad (19)$$

$$\omega_y = \dot{\theta}_y \cdot \cos(\theta_z) \cdot \cos(\theta_x) + \dot{\theta}_z \cdot \sin(\theta_x), \quad (20)$$

$$\omega_z = \dot{\theta}_z \cdot \cos(\theta_x) - \dot{\theta}_y \cdot \cos(\theta_z) \cdot \sin(\theta_x), \quad (21)$$

where ω , is the angular velocity, θ is the joint angle, and $\dot{\theta}$ is the time derivative of the joint angle.

Peak angular velocity during the reaching cycle and the percent of the reaching cycle at which peak velocity occurred was also computed. The affected arm was compared to the unaffected arm for all parameters using the Wilcoxon sign rank test.

It is difficult to identify the frequency components from the original signal, therefore, the data was evaluated in the frequency domain. The analysis included elbow angle and elbow angular velocity of the affected and unaffected arms. Converting to the frequency domain, the discrete Fourier transform of the raw signal was found by taking the 512-point fast Fourier transform (FFT). The result represents the frequency content of the signal in the range from DC up to and including the Nyquist frequency.

The spectral analysis may provide insight into elements of cocontraction, spasticity, and muscle weakness. Spectral techniques have proven useful during similar studies of electromyography (EMG) activity in which kinematics have not been described.

3. Results

3.1. Evaluation

Static linear, dynamic linear and dynamic angular evaluation was completed. Average RMS error and standard deviation results for the evaluation data was determined (Table 2).

3.2. Clinical results

The mean range of motion during the reaching tasks was determined (Fig. 4). The elbow angle for the reaching cycle of the affected and unaffected arms is displayed. The affected arms showed limited motion throughout the reaching cycle.

Mean angular velocity of the affected and unaffected arms was calculated (Fig. 5). The unaffected arms

Table 2
Validation results

Validation	Accuracy (RMS error) (%)	Standard deviation
Static linear (X-axis)	0.31	0.01 mm
Static linear (Y-axis)	0.20	0.05 mm
Static linear (Z-axis)	0.73	0.74 mm
Dynamic linear	0.36	0.85 mm
Dynamic angular	1.60	0.17°

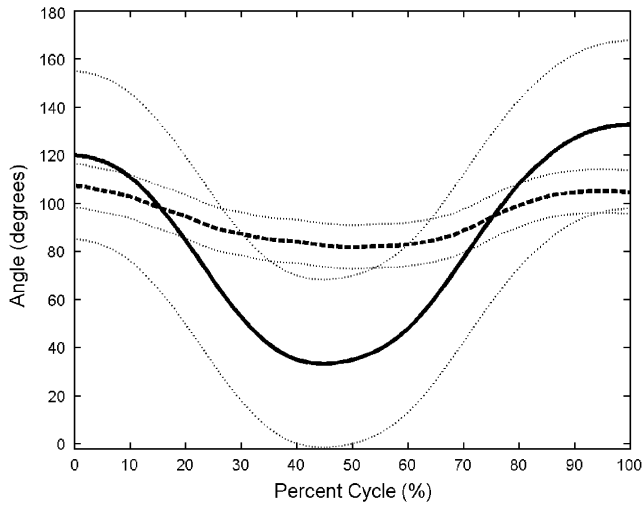


Fig. 4. Graph of the mean elbow angle and one standard deviation. Unaffected: solid, affected: dashed.

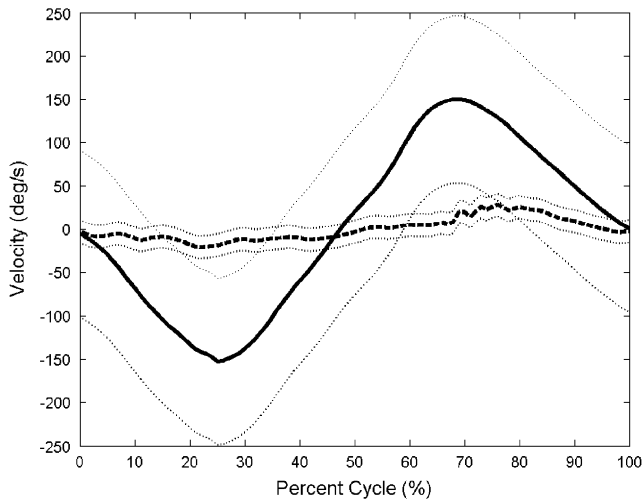


Fig. 5. Graph of the mean angular velocity of the elbow and one standard deviation. Unaffected: solid, affected: dashed.

showed a larger range of angular velocity than the affected arms, as expected.

Several parameters were computed for the affected and unaffected arms during reaching. Elbow range, peak elbow angular velocity, and the percent of the reaching cycle at which peak elbow angular velocity occurred from the affected arm was statistically tested against the unaffected arm. The Wilcoxon sign rank test was used for statistical analysis (Table 3).

Preliminary results of the frequency power spectral analysis demonstrated lower frequency content for elbow angle and angular velocity in the affected limb when compared to the unaffected limb. Frequency content for elbow angle and angular velocity of one representative patient was determined (Figs. 6 and 7).

Table 3
Wilcoxon test results

Parameter	<i>p</i> -value
Clinical flexion/extension elbow range of motion	0.01
Peak angular velocity of the clinical flexion/extension elbow angle	0.02
Percent of reaching cycle at which peak angular velocity of the clinical flexion/extension elbow angle occurred	0.55

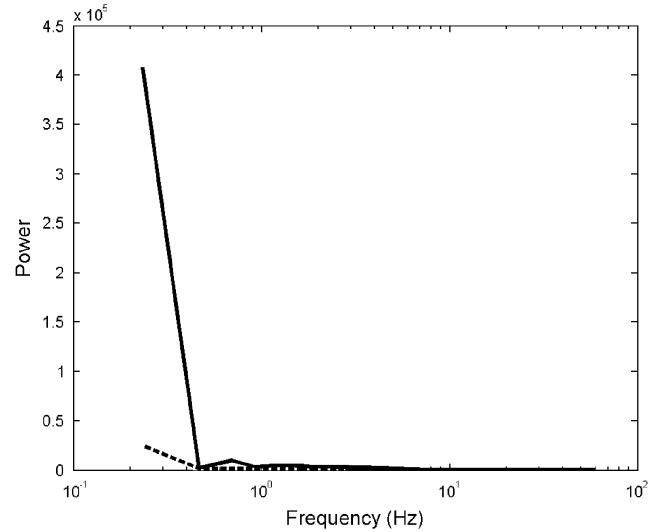


Fig. 6. Graph of the frequency content of the elbow angle (sagittal plane) from a representative subject. Unaffected: solid, affected: dashed.

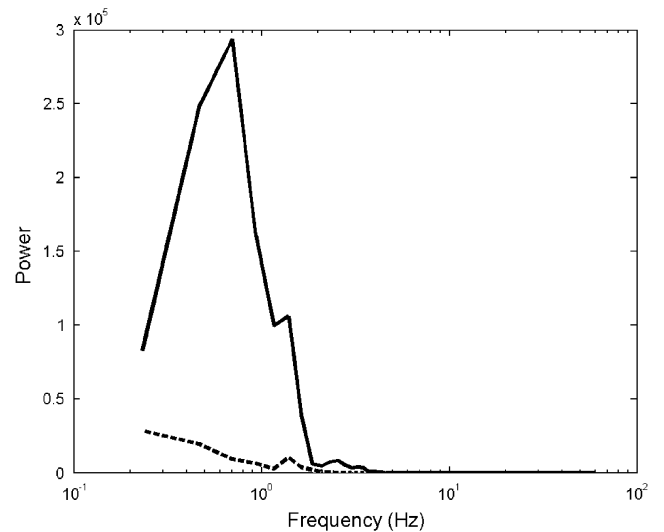


Fig. 7. Graph of the frequency content of the elbow angular velocity (sagittal plane) from a representative subject. Unaffected: solid, affected: dashed.

4. Discussion

An UE kinematic model for motion analysis is proposed. The UE is modeled with a three degree-of-freedom shoulder (glenohumeral) joint, and a two degree-of-freedom, modified hinge, elbow joint. The effectiveness of the model in detecting differences between affected and unaffected UE motion patterns of stroke was demonstrated in a population of eight patients.

The static and dynamic evaluation tests confirm the system's accuracy and precision in describing 3D upper extremity motion. The best static results are seen in the coronal and sagittal planes. The lowest average RMS error was 0.20%, along the *Y*-axis. The linear static system standard deviation was best along the *X*-axis with an average value of 0.01 mm. Results of the joint angle evaluation agreed closely with angles predicted by the earlier models of our group (Bachschmidt et al., 2001; Baker et al., 2003).

Components of the upper extremity model including segment identification and joint center locus are similar to other UE models reported in the literature. Location of the shoulder joint center, at the center of the humeral head is similar to models by Poppen, Veeger, Wang, Biryukova, Bachschmidt, Baker, and Roux (Poppen et al., 1976; Veeger et al., 1997; Wang et al., 1998; Biryukova et al., 2000; Bachschmidt et al., 2001; Roux et al., 2002; Baker et al., 2003). The design of the elbow to constrain varus and valgus is similar to the method reported by Rab and Schmidt (Schmidt et al., 1999; Rab et al., 2002). The coordinate system setup follows the general guideline described by Anglin and van der Helm (Anglin and Wyss, 2000; Wu et al., 2004).

The comparison of joint angles and angular velocities is somewhat dependent upon the performed tasks. Although the reaching-tasks slightly differ, the range of motion from the UE model agrees with that reported by Rab, Schmidt, and Yang (Schmidt et al., 1999; Rab et al., 2002; Yang et al., 2002). Several studies analyzed the tangential velocity of the UE endpoint in reaching tasks by the stroke patients (Michaelsen et al., 2001; Kamper et al., 2002). However little information is available on the UE joint velocity patterns for the stroke patients. The current model provides calculations of the joint angular velocity profile of reaching cycles.

The current model was useful in detecting significant differences between affected and unaffected metrics (range of motion, peak angular velocity). Analysis of the clinical results showed significant differences in sagittal plane range of motion and angular velocity of the elbow joint between the affected and unaffected arms during reaching tasks. The model did not detect a significant difference in the percent of the cycle at which peak velocity occurred, although a significant difference might be found with a larger subject population.

Limitations exist when using rigid-body models for analyzing human movement with surface, marker-based optical measurement systems. Considerations include relative movement of markers with respect to the underlying bony anatomy (Fuller et al., 1996; Reinschmidt, 1996; Schmidt et al., 1999; Anglin and Wyss, 2000). Other sources of error include marker placement or palpation variability, joint center identification, and link-segment anatomical description (Anglin and Wyss, 2000).

Frequency analysis at the elbow demonstrates lower spectral content in the affected arm elbow angle. The potential may exist for further characterization of task performance and pathology based on a spectral analysis concept.

References

- Adamovich, S.V., Archambault, P.S., Ghafouri, M., Levin, M.F., Poizner, H., Feldman, A.G., 2001. Hand trajectory invariance in reaching movements involving the trunk. *Experimental Brain Research* 138, 288–303.
- Andrews, J.G., Youm, Y., 1979. A biomechanical investigation of wrist kinematics. *Journal of Biomechanics* 12, 83–93.
- Anglin, C., Wyss, U.P., 2000. Review of arm motion analyses. *Institution of Mechanical Engineers* 541–555.
- Bachschmidt, R.A., Harris, G.F., Simoneau, G.G., 2001. Walker-assisted gait in rehabilitation: a study of biomechanics and instrumentation. *IEEE Transactions on Neural Systems and Rehabilitation Engineering* 9, 96–105.
- Baker, K.M., Wang, M., Cao, K., Lipsey, J., Long, J.T., Reiners, K., Johnson, C., Olson, W., Hassani, S., Ackman, J.D., Schwab, J.P., Harris, G.F., 2003. Biomechanical system for the validation of walker-assisted gait in children: design and preliminary application. *IEEE Engineering in Medicine and Biology Society*. Cancun, Mexico, 25.
- Biryukova, E.V., Roby-Brami, A., Frolov, A.A., Mokhtari, M., 2000. Kinematics of human arm reconstructed from spatial tracking system recordings. *Journal of Biomechanics* 33, 985–995.
- Chao, E.Y., 1980. Justification of triaxial goniometer for the measurement of joint rotation. *Journal of Biomechanics* 13, 989–1006.
- Fuller, J., Liu, L.J., Murphy, M.C., 1996. A comparison of lower extremity skeletal kinematics measured using skin- and pin-mounted markers. *Fourth International Symposium on 3-D Analysis of Human Movement*. University Joseph Fourier, Grenoble.
- Grood, E.S., Suntay, W.J., 1983. A joint coordinate system for the clinical description of 3-D motions: application to the knee. *Journal of Biomechanical Engineering* 105, 136–144.
- Harris, G.F., Smith, P.A., 1996. *Human Motion Analysis*. IEEE Press, New York.
- Hogfors, C., Peterson, B., Sigholm, G., Herberts, P., 1991. Biomechanical model of the human shoulder joint—II. The shoulder rhythm. *Journal of Biomechanics* 24, 699–709.
- Kamper, D.G., McKenna-Cole, A.N., Kahn, L.E., Reinkensmeyer, D.J., 2002. Alterations in reaching after stroke and their relation to movement direction and impairment severity. *Archives of Physical Medicine & Rehabilitation* 83, 702–707.
- Michaelsen, S.M., Luta, A., Roby-Brami, A., Levin, M.F., 2001. Effect of trunk restraint on the recovery of reaching movements in hemiparetic patients. *Stroke* 32, 1875–1883.

- Peterson, B., Palmerud, G., 1996. Measurement of upper extremity orientation by video stereometry system. *Medical & Biological Engineering & Computing* 34, 149–154.
- Poppen, N.K., Walker, P.S., 1976. Normal and abnormal motion of the shoulder. *Journal of Bone & Joint Surgery* 58, 195–201.
- Rab, G., Petuskey, K., Bagley, A., 2002. A method for determination of upper extremity kinematics. *Gait & Posture* 15, 113–119.
- Ramakrishnan, H.K., Kadaba, M.P., 1991. On the estimation of joint kinematics during gait. *Journal of Biomechanics* 24, 969–977.
- Rau, G., Disselhorst-Klug, C., Schmidt, R., 2000. Movement biomechanics goes upwards: from the leg to the arm. *Journal of Biomechanics* 33, 1207–1216.
- Reinschmidt, C., 1996. 3-D tibio-calcaneal and tibiofemoral kinematics during human locomotion—measured with external and bone markers. The University of Calgary, Calgary.
- Roux, E., Bouilland, S., Godillon-Maquinghen, A.P., Bouttens, D., 2002. Validation of the global optimization method within the upper limb kinematics analysis. *Journal of Biomechanics* 35, 1279–1283.
- Schmidt, R., Disselhorst-Klug, C., Silny, J., Rau, G., 1999. A marker-based measurement procedure for unconstrained wrist and elbow motions. *Journal of Biomechanics* 32, 615–621.
- Tzvetanov, P., Rousseff, R.T., Milanov, I., 2003. Lower limb SSEP changes in stroke—predictive values regarding functional recovery. *Clinical Neurology and Neurosurgery* 105, 121–127.
- Vaughan, C.L., Davis, B.L., O'Connor, J.C., 1992. *Gaitlab*. Human Kinetics Publishers, Champaign, IL.
- Veeger, H.E., Yu, B., An, K.N., Rozendal, R.H., 1997. Parameters for modeling the upper extremity. *Journal of Biomechanics* 30, 647–652.
- Wang, X., Maurin, M., Mazet, F., Maia, N.D., Voinot, K., Verriest, J.P., Fayet, M., 1998. 3-D modeling of the motion range of axial rotation of the upper arm. *Journal of Biomechanics* 31, 899–908.
- Woltring, H.J., 1986. A Fortran package for generalized, cross-validatory spline smoothing and differentiation. *Advances in Engineering Software* 8, 104–113.
- Wu, G., Helm, F.C.T.v.d., Veeger, H.E.J., Makhsous, M., van Roy, P., Anglin, C., Nagels, J., Karduna, A. R., McQuade, K., Wang, X., Werner, F. W., Buchholz, B., 2004. ISB recommendation on definitions of joint coordinate systems of various joints for the reporting of human joint motion—Part II: shoulder, elbow, wrist and hand. *Journal of Biomechanics*, in press.
- Yang, N., Zhang, M., Huang, C., Jin, D., 2002. Synergic analysis of upper limb target-reaching movements. *Journal of Biomechanics* 35, 739–746.